CMS Physics Analysis Summary

Contact: cms-pag-conveners-heavyions@cern.ch 2018/05/15

Measurement of the radial profile of D^0 mesons in jets produced in pp and PbPb collisions at 5.02 TeV

The CMS Collaboration

Abstract

The first measurement of the radial distributions of D^0 mesons in jets in PbPb and pp collisions is presented. Data samples of PbPb and pp collisions at a nucleon-nucleon center-of-mass energy of $\sqrt{s_{NN}} = 5.02$ TeV, corresponding to integrated luminosities of 404 μb^{-1} and 27.4 pb^{-1}, respectively, are recorded by the CMS detector at the LHC. The jets are reconstructed with an anti-k_T algorithm with a distance parameter of 0.3. The radial distribution of D^0 mesons with transverse momentum $p_{\mathrm{T}} > 4\,\mathrm{GeV}/c$ are measured with respect to the jet axis. Modifications of D^0 radial distribution in PbPb collisions are presented by comparing PbPb spectra to the pp reference data, indicating a redistribution of the D^0 mesons close to the jet axis. This measurement provides new experimental constraints on the mechanisms of heavy-flavor production in proton-proton collisions as well as on the processes of parton energy loss and diffusion of heavy quarks inside the strongly interacting medium produced in heavy ion collisions.

The production of quarks and gluons in hard parton scatterings in relativistic heavy ion collisions provides useful probes of the quark-gluon plasma (QGP), a deconfined state of quarks and gluons [1, 2]. The outgoing partons, which produce final-state jets of particles, interact strongly with the QGP and lose energy [3–11] through jet quenching, a phenomenon observed at RHIC [12, 13] and the LHC [14–18]. The modifications of jet energy and structure can be related, via theoretical models, to the thermodynamical and transport properties of the medium [9–11, 19–21]. One of the most striking features of the jet quenching is the enhanced production of low transverse momentum (p_{T}) hadrons at large angles with respect to the final-state jet axis. This phenomenon is observed as modifications of the jet fragmentation [22, 23], the modification of the jet radial profile and energy flow [24, 25]. Interpretations of those experimental results include medium-induced gluon radiation, modification of jet splitting functions, and medium response to the hard scattered partons [11, 26–29]. By studying the associated hadrons with different masses, one could gain insights into the origin of the enhanced production of the low p_{T} charged particles in jets.

In addition to the motivation stated above, measurements of the heavy flavor meson production in jets could provide new information about heavy flavor jet fragmentation in both pp and PbPb collisions. Moreover, heavy flavor meson+jet correlation measurements could be used to constrain parton energy loss mechanisms and to measure the heavy quark diffusion inside the medium [30–32], complementary to the measurements of inclusive heavy flavor meson spectra [33–37], heavy flavor meson azimuthal anisotropy [37–41], and heavy flavor tagged jets [42, 43].

Studies of D^0 + jet correlations become feasible for the first time with high statistics PbPb collisions delivered by the Large Hadron Collider in 2015. In this Letter, the first measurement of the radial distributions of D^0 mesons in jets in PbPb and pp collisions with the CMS detector is presented. The observable is the angular distribution of the D^0 meson with respect to the jet axis, defined as

$$\frac{1}{N_{\mathrm{JD}}}\frac{dN_{\mathrm{JD}}}{dr} = \frac{1}{N_{\mathrm{JD}}\Delta r}\frac{N_{\mathrm{JD}}|_{\Delta r}}{(\alpha \times \epsilon)} \tag{1}$$

where $r = \sqrt{\Delta\phi_{\mathrm{JD}}^2 + \Delta\eta_{\mathrm{JD}}^2}$ is defined by relative pseudorapidity ($\Delta\eta_{\mathrm{JD}}$) and relative azimuth ($\Delta\phi_{\mathrm{JD}}$) of D^0 from the jet axis, and Δr is the width of the r interval. $\alpha \times \epsilon$ represents the acceptance times efficiency correction applied, $N_{\mathrm{JD}}|_{\Delta r}$ is the number of signal D^0 in the Δr interval, and N_{JD} is the integral of the distribution in the r region from 0 to 0.3.

The main feature of the CMS detector is a superconducting solenoid, providing a magnetic field of 3.8 T. Within the solenoid volume are a silicon pixel and strip tracker which is used to detect charged particles, a lead tungstate crystal electromagnetic calorimeter (ECAL), and a brass and scintillator hadron calorimeter (HCAL), each composed of a barrel and two endcap sections. Hadron forward (HF) calorimeters extend the pseudorapidity coverage up to $|\eta| = 5.2$ and are used for collision event selection. Muons are detected in gas-ionization chambers embedded in the steel flux-return yoke outside the solenoid, which are used in the jet reconstruction. A more detailed description of the CMS detector, together with a definition of the coordinate system used and the relevant kinematic variables, can be found in Ref. [44].

The pp (PbPb) dataset used for this analysis corresponds to an integrated luminosity of 27.4 pb^{-1} (404 $\mu\mathrm{b}^{-1}$). High p_{T} jet events were selected by high-level trigger (HLT) algorithms, with $p_{\mathrm{T}}^{\mathrm{jet}}$ threshold 60 GeV/c. For the offline analysis, events have to pass a set of selection criteria

designed to reject events from background processes (beam-gas collisions and beam scraping events) as described in Ref. [45, 46].

Several Monte Carlo (MC) simulated event samples are used to evaluate the background contributions, signal efficiencies, and detector acceptance corrections. The events produced include both prompt (produced directly from c-quark fragmentation) and nonprompt (from b hadron decays) D^0 meson events. Proton-proton collisions are generated with PYTHIA 8 v212 [47] tune CUETP8M1 [48] and propagated through the CMS detector using the GEANT4 package [49]. EVTGEN 1.3.0 [50] is used to simulate D^0 meson decays, and final-state photon radiation in the D^0 decays is simulated with PHOTOS 2.0 [51]. For the PbPb MC samples, each PYTHIA 8 event is embedded into a PbPb collision event generated with HYDJET 1.8 [52], which is tuned to reproduce global event properties such as the underlying event p_T density, charged-hadron p_T spectrum and particle multiplicity.

The particle-flow (PF) algorithm [53] is used for the jet reconstruction with the anti-k_T algorithm provided in the FASTJET framework [54, 55] with a distance parameter $R = 0.3$ chosen to minimize the effects of the underlying event (UE) fluctuations. The PF algorithm aims to reconstruct and identify each individual particle in an event, with an optimized combination of information from the various elements of the CMS detector. The energy of photons is directly obtained from the ECAL measurement, corrected for zero-suppression effects. The energy of electrons is determined from a combination of the electron momentum at the primary interaction vertex as determined by the tracker, the energy of the corresponding ECAL cluster, and the energy sum of all bremsstrahlung photons spatially compatible with originating from the electron track. The energy of muons is obtained from the curvature of the corresponding track. The energy of charged hadrons is determined from a combination of their momentum measured in the tracker and the matching ECAL and HCAL energy deposits, corrected for zero-suppression effects and for the response function of the calorimeters to hadronic showers. Finally, the energy of neutral hadrons is obtained from the corresponding corrected ECAL and HCAL energy. In order to subtract the UE background in PbPb collisions, an iterative algorithm [56] is employed [15, 16]. In pp collisions, where the UE level is negligible, jets are reconstructed without UE subtraction. The jet energy corrections are derived from simulation, separately for pp and PbPb, and are confirmed via energy-balance methods applied to dijet and photon+jet events in pp data [57]. Jets with $|\eta^{\mathrm{jet}}| < 1.6$ and corrected $p_{\mathrm{T}}^{\mathrm{jet}} > 60\,\mathrm{GeV}/c$ are selected for correlation analyses.

The D^0 candidates are reconstructed by combining pairs of oppositely charged particle tracks with an invariant mass within 0.2 GeV/c^2 of the world-average D^0 mass [58]. Each track is required to have $p_T > 2\,\mathrm{GeV}/c$ in order to reduce the combinatorial background. All tracks are also required to be within $|\eta| < 2$, and pass a set of quality selections [45]. For each pair of selected tracks, two D^0 candidates are created by assuming that one of the particles has the mass of the pion while the other has the mass of the kaon, and vice-versa. The D^0 mesons are required to be within rapidity $|y| < 2$ and $p_{\mathrm{T}}^{\mathrm{D}} > 4\,\mathrm{GeV}/c$. In order to further reduce the combinatorial background, the D^0 candidates are selected based on three topological criteria: on the three-dimensional decay length (distance between primary vertex and D^0 secondary vertex) $L_{3\mathrm{D}}$ normalized to its uncertainty (required to be larger than 2.34–4.00), on the pointing angle θ_{p} (defined as the angle between the total momentum vector of the tracks and the vector connecting the primary and the secondary vertices and required to be smaller than 0.020–0.046), and on the χ^2 probability of the D^0 vertex fit (required to be larger than 5%).

The measured radial distributions are presented in two $p_{\mathrm{T}}^{\mathrm{D}}$ bins, $4 < p_{\mathrm{T}}^{\mathrm{D}} < 20\,\mathrm{GeV}/c$ and $p_{\mathrm{T}}^{\mathrm{D}} > 20\,\mathrm{GeV}/c$, and four r bins, 0–0.05, 0.05–0.1, 0.1–0.3, and 0.3–0.5. The D^0 meson yield in

each p_T and r interval is extracted with a binned maximum-likelihood fit to the invariant mass distributions in the range $1.7 < m_{\pi K} < 2.0$ GeV/c^2. The combinatorial background, originating from random pairs of tracks not produced by a D^0 meson decay, is modeled by a third-order polynomial. The signal shape was found to be best modeled over the entire p_T range measured by sum of two Gaussian functions with the same mean but different widths. An additional Gaussian function with much wider width is used to describe the invariant mass shape of D^0 candidates with incorrect mass assignment from the exchange of the pion and kaon designations. The widths of the Gaussian functions that describe the D^0 signal shape and the shape of the D^0 candidates with swapped mass assignments are fixed from simulation with different resolution between MC and data taken into account. Also, the ratio between the numbers of the signal and of the D^0 candidates with swapped mass assignments is fixed to the value extracted from simulation. No significant variations in the shape of the combinatorial background and in the mean and the σ of the distributions of signal D^0 mesons and of D^0 candidates with swapped mass hypothesis in the different r-intervals of the analysis were observed.

The D^0 yields are corrected for detector acceptance, trigger, track reconstruction, and selection inefficiencies in bins of p_T^D and r. The correction factors are obtained from a PYTHIA (PYTHIA+HYDJET) MC sample for pp (PbPb) analysis. In this analysis, the background contribution coming from pairs formed by a combining a D^0 meson with a jet not coming from the same hard scattering or with a fake jet is subtracted using an event mixing technique. This background is estimated by combining the distributions of D^0-jet pairs formed with jets from the signal event and D^0 mesons from minimum-bias (MB) events, jets from MB events with D^0 mesons from the signal event, and jets and D^0 mesons from MB events. The background distribution is then subtracted from the raw D^0 radial distribution measured in the signal event. In this procedure, each signal event is mixed with a minimum-bias event which presents a similar primary vertex position, HF energy and an event plane angle. The event plane is an experimental estimation of the reaction plane, defined by the beam direction and the impact parameter vector between two colliding nuclei. It is determined from the two HF calorimeters covering the range $3 < |\eta| < 5$ [59]. Finally, the background subtracted jet shape distribution is corrected for jet resolution effects using a bin-by-bin correction, which is obtained from PYTHIA+HYDJET MC.

Several sources of systematic uncertainty are considered for the D^0 yield extraction and the jet reconstruction which are studied in bins of p_T^D and r. The uncertainty in the raw yield extraction (2.6–5.4% for pp and 1.4–8.2% for PbPb data) is evaluated by repeating the fit procedure using different background and signal fit functions and by varying the widths of the Gaussian functions that describe the D^0 signal according to differences between data and MC. In the signal variation study, the sum of three Gaussian functions with the same mean but different widths is considered, while in the background variation study, a second-order polynomial function is used. This functional form provides a good description of the combinatorial background according to same-sign studies. The systematic uncertainty due to the selection of the D^0 meson candidates (3.6% and 0.5% for the low and high-p_T^D bin, respectively, for pp and 3.5% and 2.7% for PbPb data) is estimated by considering the differences between MC and data in the reduction of the D^0 yields obtained by applying each of the D^0 selection variables. The study is performed by varying one selection at a time in a range that allowed a robust signal extraction procedure and by considering the maximum relative discrepancy in the yield reduction between data and MC. The total uncertainty is the quadratic sum of the maximum relative discrepancy obtained by varying each of the three selection variables separately.

The systematic uncertainties for the jets used in the analysis include components for the uncertainty in jet energy scale (JES) and jet energy resolution (JER). The systematic uncertainty

pertaining to JES is estimated by varying the $p_{\mathrm{T}}^{\mathrm{jet}}$ by 2.8% (in both pp and PbPb results), which represents the sum in quadrature of the observed data-MC differences (2%) and the non-closure (i.e. deviation from unity) in MC, when comparing reconstructed (detector level) jets versus truth (generator level) jets smeared by the known detector and reconstruction effects. An additional uncertainty (1.6%–17.5% for pp and 1.8%–41.8% for PbPb) is added to account for the different detector response to quark versus gluon jets. The assigned uncertainty represents the maximum difference from the nominal results, when applying JES corrections obtained with a pure-gluon sample or a pure-quark sample.

The systematic uncertainty for the JER is estimated by varying by 15% the $p_{\mathrm{T}}^{\mathrm{jet}}$ energy resolution to account for an imperfect description of the fluctuations of the UE event in MC simulations. The variation considered is estimated by studying the effects of these fluctuations using two different methods: the random cone technique [57, 60] and the embedding procedure. The random cone method consists of reconstructing many jets in a zero bias event, clustering particles in randomly placed cones in the entire (η, ϕ) space. When the method is applied in events with no contribution from hard scatterings, as it is the case for zero-bias events, the standard deviation of the distribution of the jet p_{T} obtained with this procedure can be indeed used to estimate the magnitude of the UE fluctuations.

The relative variations in the results are 0.3%–3.0% in pp, and 0.6%–5.6% in PbPb. Also, the systematic uncertainties from trigger bias is estimated by the difference between the result with trigger efficiency corrected and the nominal result, which are 0.3%–2.7% in pp and 0.7%–14.5% in PbPb. Finally, since a bin-by-bin correction is applied for the non-closure between reconstructed and generated jets smeared by the resolution extracted from simulation, the magnitude of the correction is quoted as the systematic uncertainties for resolution unfolding, which are between 1.3%–30.7% in pp and 0.7%-31.5% in PbPb.

Figure 1 shows the measured D^0 radial distributions in pp and PbPb collisions. The results are compared to predictions from the PYTHIA 8 event generator. At low D^0 p_{T} ($4 < p_{\mathrm{T}}^{\mathrm{D}} < 20\,\mathrm{GeV}/c$), the measured spectrum in pp collisions reaches a maximum at $0.05 < r < 0.1$, consistent with the prediction from PYTHIA 8 for pp events. A hint that the predictions from PYTHIA 8 produce a too wide radial profile is observed for low p_{T} D^0 mesons. To measure the modification of the radial profile, a ratio of PbPb to pp spectra is also presented. This ratio increases as a function of r. This result could indicate that D^0 mesons at low p_{T} are farther away from the jet axis in PbPb compared to pp collisions. At high D^0 p_{T} ($p_{\mathrm{T}}^{\mathrm{D}} > 20\,\mathrm{GeV}/c$), the measured spectra in pp and PbPb collisions fall rapidly as a function of r, similarly to what was observed in inclusive jet-hadron correlation functions [61]. The ratio of PbPb to pp is consistent with unity within uncertainties, which could indicate that the modification of the radial profile of high-p_{T} D^0 mesons is small.

In summary, the first measurement of the radial distributions of D^0 mesons in jets in PbPb and pp collisions is performed with the CMS detector using jets with $p_{\mathrm{T}} > 60\,\mathrm{GeV}/c$ and D^0 mesons with $p_{\mathrm{T}} > 4\,\mathrm{GeV}/c$. The modification of the D^0 radial distributions in PbPb collisions are studied by comparing the PbPb spectra to the pp reference data. The measurements indicate a modification of the D^0 radial profile in PbPb collisions at low D^0 p_{T} that vanishes at higher D^0 p_{T}. This measurement provides new experimental constraints on the mechanisms of heavy-flavor production in proton-proton collisions as well as on the processes of parton energy loss and diffusion of heavy quarks inside the quark-gluon plasma.

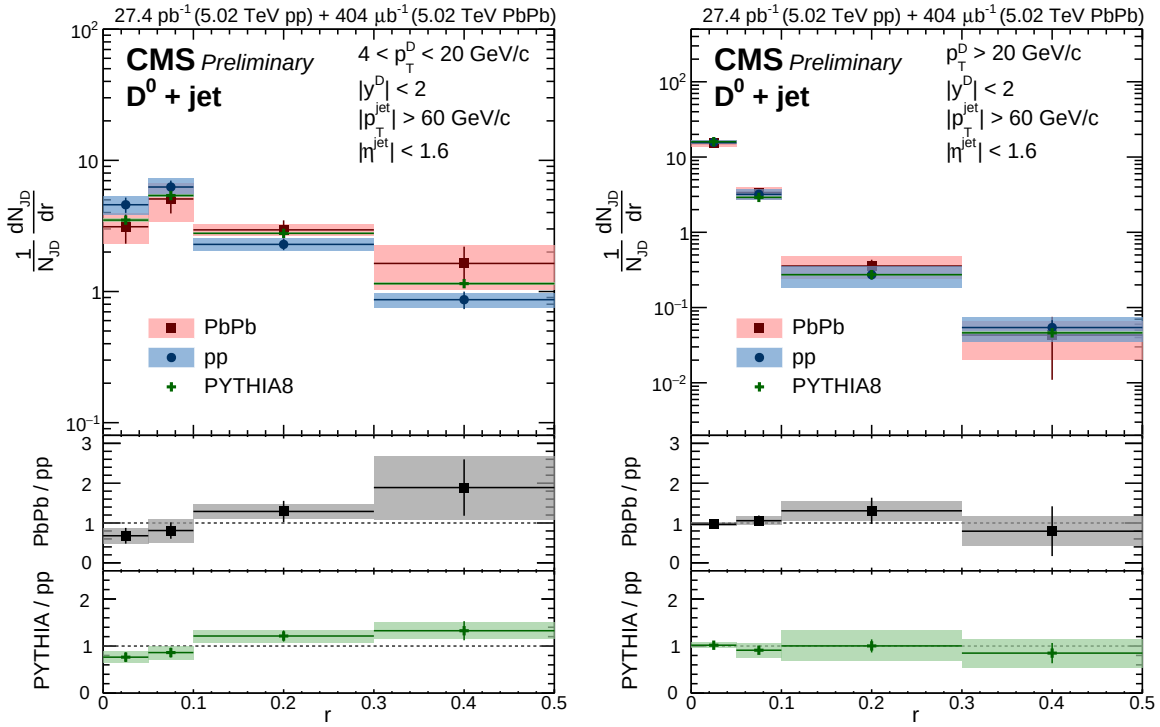

Figure 1: Distributions of D^0 mesons in jets as a function of the distance from the jet axis for jets of $p_{\mathrm{T}}^{\mathrm{jet}}$ >60 GeV/c and $|\eta^{\mathrm{jet}}|$ <1.6 measured in pp and PbPb collisions at $\sqrt{s_{NN}} = 5.02$ TeV. The measurement is performed in the D^0 $p_{\mathrm{T}}^{\mathrm{D}}$ range 4–20 GeV/c (left) and for $p_{\mathrm{T}}^{\mathrm{D}}$ >20 GeV/c (right). Each spectrum is normalized to its integral in the region 0< r <0.3. The vertical bars (boxes) correspond to statistical (systematic) uncertainties. The ratios of the D^0 radial distributions of PbPb to pp are also presented in the middle panel of each figure. The predictions from the PYTHIA 8 event generator are also superimposed, and in the bottom panel the ratios of the D^0 radial distributions of pp over PYTHIA 8 predictions are presented.

References

[1] E. V. Shuryak, "Quark-Gluon Plasma and hadronic production of leptons, photons and pions", *Phys. Lett. B* **78** (1978) 150, doi:10.1016/0370-2693(78)90370-2.

[2] E. V. Shuryak, "What RHIC experiments and theory tell us about properties of quark-gluon plasma?", *Nucl. Phys. A* **750** (2005) 64, doi:10.1016/j.nuclphysa.2004.10.022, arXiv:hep-ph/0405066.

[3] D. A. Appel, "Jets as a probe of quark-gluon plasmas", *Phys. Rev. D* **33** (1986) 717, doi:10.1103/PhysRevD.33.717.

[4] J. P. Blaizot and L. D. McLerran, "Jets in expanding quark-gluon plasmas", *Phys. Rev. D* **34** (1986) 2739, doi:10.1103/PhysRevD.34.2739.

[5] M. Gyulassy and M. Plumer, "Jet quenching in dense matter", *Phys. Lett. B* **243** (1990) 432, doi:10.1016/0370-2693(90)91409-5.

[6] X.-N. Wang and M. Gyulassy, "Gluon shadowing and jet quenching in $A + A$ collisions at $\sqrt{s} = 200A$ GeV", *Phys. Rev. Lett.* **68** (1992) 1480, doi:10.1103/PhysRevLett.68.1480.

[7] R. Baier et al., "Radiative energy loss and p_{T} broadening of high-energy partons in nuclei", *Nucl. Phys. B* **484** (1997) 265, doi:10.1016/S0550-3213(96)00581-0, arXiv:hep-ph/9608322.

[8] B. G. Zakharov, "Radiative energy loss of high-energy quarks in finite-size nuclear matter and quark-gluon plasma", *JETP Lett.* **65** (1997) 615, doi:10.1134/1.567389, arXiv:hep-ph/9704255.

[9] J. Casalderrey-Solana and C. A. Salgado, "Introductory lectures on jet quenching in heavy ion collisions", *Acta Phys. Polon. B* **38** (2007) 3731, arXiv:0712.3443.

[10] D. d'Enterria, "Jet quenching", in *Relativistic Heavy Ion Physics*, R. Stock, ed., volume 23, p. 99. Springer-Verlag Berlin Heidelberg, 2010. arXiv:0902.2011. Landolt-Börnstein/SpringerMaterials. doi:10.1007/978-3-642-01539-7_16.

[11] U. A. Wiedemann, "Jet quenching in heavy ion collisions", *Landolt-Bornstein* (2010) 521, doi:10.1007/978-3-642-01539-7_17, arXiv:0908.2306.

[12] STAR Collaboration, "Direct observation of dijets in central Au + Au collisions at $\sqrt{s_{NN}} = 200\,\mathrm{GeV}$", *Phys. Rev. Lett.* **97** (2006) 162301, doi:10.1103/PhysRevLett.97.162301, arXiv:nucl-ex/0604018.

[13] PHENIX Collaboration, "Transverse momentum and centrality dependence of dihadron correlations in Au+Au collisions at $\sqrt{s_{\mathrm{NN}}} = 200$ gev: Jet quenching and the response of partonic matter", *Phys. Rev. C* **77** (2008) 011901, doi:10.1103/PhysRevC.77.011901, arXiv:0705.3238.

[14] ATLAS Collaboration, "Observation of a centrality-dependent dijet asymmetry in lead-lead collisions at $\sqrt{s_{\mathrm{NN}}} = 2.76\,\mathrm{TeV}$ with the ATLAS detector at the LHC", *Phys. Rev. Lett.* **105** (2010) 252303, doi:10.1103/PhysRevLett.105.252303, arXiv:1011.6182.

[15] CMS Collaboration, "Observation and studies of jet quenching in PbPb collisions at $\sqrt{s_{\mathrm{NN}}} = 2.76\,\mathrm{TeV}$", *Phys. Rev. C* **84** (2011) 024906, doi:10.1103/PhysRevC.84.024906, arXiv:1102.1957.

[16] CMS Collaboration, "Jet momentum dependence of jet quenching in PbPb collisions at $\sqrt{s_{\mathrm{NN}}} = 2.76\,\mathrm{TeV}$", *Phys. Lett. B* **712** (2012) 176, doi:10.1016/j.physletb.2012.04.058, arXiv:1202.5022.

[17] CMS Collaboration, "Studies of jet quenching using isolated-photon + jet correlations in PbPb and pp collisions at $\sqrt{s_{\mathrm{NN}}} = 2.76$ TeV", *Phys. Lett. B* **718** (2013) 773, doi:10.1016/j.physletb.2012.11.003, arXiv:1205.0206.

[18] ALICE Collaboration, "Measurement of jet suppression in central Pb–Pb collisions at $\sqrt{s_{\mathrm{NN}}} = 2.76$ TeV", *Phys. Lett. B* **746** (2015) 1, doi:10.1016/j.physletb.2015.04.039, arXiv:1502.01689.

[19] J. Casalderrey-Solana, Y. Mehtar-Tani, C. A. Salgado, and K. Tywoniuk, "New picture of jet quenching dictated by color coherence", *Phys. Lett.* **725** (2013) 357, doi:10.1016/j.physletb.2013.07.046, arXiv:1210.7765.

[20] JET Collaboration, "Extracting the jet transport coefficient from jet quenching in high-energy heavy-ion collisions", *Phys. Rev. C* **90** (2014) 014909, doi:10.1103/PhysRevC.90.014909, arXiv:1312.5003.

[21] J. Casalderrey-Solana et al., "A hybrid strong/weak coupling approach to jet quenching", *JHEP* **10** (2014) 019, doi:10.1007/JHEP10(2014)019, arXiv:1405.3864.

[22] CMS Collaboration, "Measurement of jet fragmentation in PbPb and pp collisions at $\sqrt{s_{\rm NN}} = 2.76$ TeV", *Phys. Rev. C* **90** (2014) 024908, doi:10.1103/PhysRevC.90.024908, arXiv:1406.0932.

[23] ATLAS Collaboration, "Measurement of jet fragmentation in Pb+Pb and pp collisions at $\sqrt{s_{\rm NN}} = 2.76$ TeV with the ATLAS detector at the LHC", *Eur. Phys. J. C* **77** (2017) 379, doi:10.1140/epjc/s10052-017-4915-5, arXiv:1702.00674.

[24] CMS Collaboration, "Modification of jet shapes in PbPb collisions at $\sqrt{s_{\rm NN}} = 2.76$ TeV", *Phys. Lett. B* **730** (2014) 243, doi:10.1016/j.physletb.2014.01.042, arXiv:1310.0878.

[25] CMS Collaboration, "Measurement of transverse momentum relative to dijet systems in PbPb and pp collisions at $\sqrt{s_{\rm NN}} = 2.76$ TeV", *JHEP* **01** (2016) 006, doi:10.1007/JHEP01(2016)006, arXiv:1509.09029.

[26] J. Casalderrey-Solana and C. A. Salgado, "Introductory lectures on jet quenching in heavy ion collisions", *Acta Phys. Polon. B* **38** (2007) 3731, arXiv:0712.3443.

[27] D. d'Enterria, "Jet quenching", in *Springer Materials - The Landolt-Börnstein Database*, R. Stock, ed., volume 23: Relativistic Heavy Ion Physics, p. 99. Springer-Verlag, 2010. arXiv:0902.2011. doi:10.1007/978-3-642-01539-7_16.

[28] A. Majumder and M. Van Leeuwen, "The theory and phenomenology of perturbative QCD based jet quenching", *Prog. Part. Nucl. Phys.* **66** (2011) 41, doi:10.1016/j.ppnp.2010.09.001, arXiv:1002.2206.

[29] JET Collaboration, "Extracting the jet transport coefficient from jet quenching in high-energy heavy-ion collisions", *Phys. Rev. C* **90** (2014) 014909, doi:10.1103/PhysRevC.90.014909, arXiv:1312.5003.

[30] M. Nahrgang, J. Aichelin, P. B. Gossiaux, and K. Werner, "Azimuthal correlations of heavy quarks in Pb + Pb collisions at $\sqrt{s} = 2.76$ TeV at the CERN Large Hadron Collider", *Phys. Rev.* **C90** (2014), no. 2, 024907, doi:10.1103/PhysRevC.90.024907, arXiv:1305.3823.

[31] S. Cao, G.-Y. Qin, and S. A. Bass, "Modeling of heavy-flavor pair correlations in Au-Au collisions at 200A GeV at the BNL Relativistic Heavy Ion Collider", *Phys. Rev.* **C92** (2015), no. 5, 054909, doi:10.1103/PhysRevC.92.054909, arXiv:1505.01869.

[32] R. Hambrock and W. A. Horowitz, "AdS/CFT predictions for azimuthal and momentum correlations of $b\bar{b}$ pairs in heavy ion collisions", *Nucl. Part. Phys. Proc.* **289-290** (2017) 233–236, doi:10.1016/j.nuclphysbps.2017.05.052, arXiv:1703.05845.

[33] ALICE Collaboration, "Transverse momentum dependence of D-meson production in Pb-Pb collisions at $\sqrt{s_{\rm NN}} = 2.76$ TeV", *JHEP* **03** (2016) 081, doi:10.1007/JHEP03(2016)081, arXiv:1509.06888.

[34] ALICE Collaboration, "Centrality dependence of high-p_T D meson suppression in Pb-Pb collisions at $\sqrt{s_{\rm NN}} = 2.76$ TeV", *JHEP* **11** (2015) 205, doi:10.1007/JHEP11(2015)205, arXiv:1506.06604. [Erratum: doi:10.1007/JHEP06(2017)032].

[35] CMS Collaboration, "Nuclear modification factor of D0 mesons in PbPb collisions at $\sqrt{s_{\mathrm{NN}}}$ = 5.02 TeV", arXiv:1708.04962.

[36] CMS Collaboration, "Measurement of the $B^{\pm}$ Meson Nuclear Modification Factor in Pb-Pb Collisions at $\sqrt{s_{NN}} = 5.02$ TeV", *Phys. Rev. Lett.* **119** (2017), no. 15, 152301, doi:10.1103/PhysRevLett.119.152301, arXiv:1705.04727.

[37] CMS Collaboration, "Suppression and azimuthal anisotropy of prompt and nonprompt J/ψ production in PbPb collisions at $\sqrt{s_{\mathrm{NN}}} = 2.76$ TeV", *Eur. Phys. J. C* **77** (2017) 252, doi:10.1140/epjc/s10052-017-4781-1, arXiv:1610.00613.

[38] ALICE Collaboration, "Azimuthal anisotropy of D meson production in Pb-Pb collisions at $\sqrt{s_{\mathrm{NN}}} = 2.76$ TeV", *Phys. Rev.* **C90** (2014), no. 3, 034904, doi:10.1103/PhysRevC.90.034904, arXiv:1405.2001.

[39] CMS Collaboration, "Measurement of prompt D^0 meson azimuthal anisotropy in PbPb collisions at $\sqrt{s_{NN}}$ = 5.02 TeV", arXiv:1708.03497.

[40] STAR Collaboration, "Measurement of D^0 Azimuthal Anisotropy at Midrapidity in Au+Au Collisions at $\sqrt{s_{\mathrm{NN}}}$=200 GeV", *Phys. Rev. Lett.* **118** (2017), no. 21, 212301, doi:10.1103/PhysRevLett.118.212301, arXiv:1701.06060.

[41] ALICE Collaboration, "D-meson azimuthal anisotropy in midcentral Pb-Pb collisions at $\sqrt{\mathbf{s}_{\mathrm{NN}}} = \mathbf{5.02}$ TeV", *Phys. Rev. Lett.* **120** (2018), no. 10, 102301, doi:10.1103/PhysRevLett.120.102301, arXiv:1707.01005.

[42] CMS Collaboration, "Evidence of b-Jet Quenching in PbPb Collisions at $\sqrt{s_{\mathrm{NN}}} = 2.76$ TeV", *Phys. Rev. Lett.* **113** (2014), no. 13, 132301, doi:10.1103/PhysRevLett.115.029903, 10.1103/PhysRevLett.113.132301, arXiv:1312.4198. [Erratum: Phys. Rev. Lett.115,no.2,029903(2015)].

[43] CMS Collaboration, "Comparing transverse momentum balance of b jet pairs in pp and PbPb collisions at $\sqrt{s_{\mathrm{NN}}} = 5.02$ TeV", arXiv:1802.00707.

[44] CMS Collaboration, "The CMS experiment at the CERN LHC", *JINST* **3** (2008) S08004, doi:10.1088/1748-0221/3/08/S08004.

[45] CMS Collaboration, "Charged-particle nuclear modification factors in PbPb and pPb collisions at $\sqrt{s_{\mathrm{NN}}} = 5.02$ TeV", *JHEP* **04** (2017) 039, doi:10.1007/JHEP04(2017)039, arXiv:1611.01664.

[46] CMS Collaboration, "Transverse momentum and pseudorapidity distributions of charged hadrons in pp collisions at $\sqrt{s} = 0.9$ and 2.36 TeV", *JHEP* **02** (2010) 041, doi:10.1007/JHEP02(2010)041, arXiv:1002.0621.

[47] T. Sjöstrand et al., "An Introduction to PYTHIA 8.2", *Comput. Phys. Commun.* **191** (2015) 159, doi:10.1016/j.cpc.2015.01.024, arXiv:1410.3012.

[48] CMS Collaboration, "Event generator tunes obtained from underlying event and multiparton scattering measurements", *Eur. Phys. J. C* **76** (2016) 155, doi:10.1140/epjc/s10052-016-3988-x, arXiv:1512.00815.

[49] GEANT4 Collaboration, "GEANT4 — a simulation toolkit", *Nucl. Instrum. Meth. A* **506** (2003) 250, doi:10.1016/S0168-9002(03)01368-8.

[50] D. J. Lange, "The EvtGen particle decay simulation package", *Nucl. Instrum. Meth. A* **462** (2001) 152, doi:10.1016/S0168-9002(01)00089-4.

[51] E. Barberio, B. van Eijk, and Z. Was, "Photos – a universal Monte Carlo for QED radiative corrections in decays", *Comput. Phys. Commun.* **66** (1991) 115, doi:10.1016/0010-4655(91)90012-A.

[52] I. P. Lokhtin and A. M. Snigirev, "A model of jet quenching in ultrarelativistic heavy ion collisions and high-p_{T} hadron spectra at RHIC", *Eur. Phys. J. C* **45** (2006) 211, doi:10.1140/epjc/s2005-02426-3, arXiv:hep-ph/0506189.

[53] CMS Collaboration, "Particle-flow reconstruction and global event description with the cms detector", *JINST* **12** (2017) P10003, doi:10.1088/1748-0221/12/10/P10003, arXiv:1706.04965.

[54] M. Cacciari, G. P. Salam, and G. Soyez, "The anti-k_t jet clustering algorithm", *JHEP* **04** (2008) 063, doi:10.1088/1126-6708/2008/04/063, arXiv:0802.1189.

[55] M. Cacciari, G. P. Salam, and G. Soyez, "FastJet user manual", *Eur. Phys. J. C* **72** (2012) 1896, doi:10.1140/epjc/s10052-012-1896-2, arXiv:1111.6097.

[56] O. Kodolova, I. Vardanian, A. Nikitenko, and A. Oulianov, "The performance of the jet identification and reconstruction in heavy ions collisions with CMS detector", *Eur. Phys. J. C* **50** (2007) 117, doi:10.1140/epjc/s10052-007-0223-9.

[57] CMS Collaboration, "Jet energy scale and resolution in the CMS experiment in pp collisions at 8 TeV", *JINST* **12** (2017) P02014, doi:10.1088/1748-0221/12/02/P02014, arXiv:1607.03663.

[58] Particle Data Group, C. Patrignani et al., "Review of Particle Physics", *Chin. Phys. C* **40** (2016), no. 10, 100001, doi:10.1088/1674-1137/40/10/100001.

[59] CMS Collaboration Collaboration, "Measurement of the elliptic anisotropy of charged particles produced in pbpb collisions at $\sqrt{s_{NN}} = 2.76$ tev", *Phys. Rev. C* **87** (Jan, 2013) 014902, doi:10.1103/PhysRevC.87.014902.

[60] CMS Collaboration Collaboration, "Measurement of inclusive jet cross sections in pp and pbpb collisions at $\sqrt{s_{\mathrm{NN}}} = 2.76$ tev", *Phys. Rev. C* **96** (Jul, 2017) 015202, doi:10.1103/PhysRevC.96.015202.

[61] CMS Collaboration, "Jet properties in PbPb and pp collisions at $\sqrt{s_{\mathrm{NN}}} = 5.02$ TeV", arXiv:1803.00042.